

De-Anonymizing Text by Fingerprinting Language Generation

Zhen Sun
Cornell University
zs352@cornell.edu

Roei Schuster
Tel Aviv University
Cornell Tech
rs864@cornell.edu

Vitaly Shmatikov
Cornell Tech
shmat@cs.cornell.edu

Abstract

Components of machine learning systems are not (yet) perceived as security hotspots. Secure coding practices, such as ensuring that no execution paths depend on confidential inputs, have not yet been adopted by ML developers. We initiate the study of code security of ML systems by investigating how nucleus sampling—a popular approach for generating text, used for applications such as auto-completion—unwittingly leaks texts typed by users. Our main result is that the series of nucleus sizes for many natural English word sequences is a unique *fingerprint*. We then show how an attacker can infer typed text by measuring these fingerprints via a suitable side channel (e.g., cache access times), explain how this attack could help de-anonymize anonymous texts, and discuss defenses.

1 Introduction

Machine learning (ML) models are composed from building blocks such as layer types, loss functions, sampling methods, etc. Each building block typically has a few popular library implementations, which are incorporated into many models—including models whose inputs are sensitive (e.g., private images or typed text). Therefore, ML models are “security hotspots” and their implementations must follow secure coding practices. This includes protecting the inputs from *side channels*, i.e., low-level physical or microarchitectural “side effects” of the computation that are externally observable and leak information about its internal state to concurrent, adversarial processes.

We use *nucleus sampling* [19], a leading approach for efficiently generating high-fidelity text, as a case study of side-channel vulnerabilities in ML models. Given the output probabilities of a language model such as GPT-2 [34], nucleus sampling draws candidates from a variable-sized “nucleus” of most probable words. It is the basis of applications such as text auto-completion [24, 42].

First, we demonstrate that *the series of nucleus sizes produced when generating an English-language word sequence is a fingerprint* by showing that the nucleus size series

of any sequence satisfying a simple criterion is far from any other sequence, unless their textual contents substantially overlap. We then derive a lower bound on the Euclidean distance between fingerprints that depends only on the sequence length but not on the size or domain of the corpus.

Second, we show that implementations of nucleus sampling, such as the popular Hugging Face transformers package, contain a dangerous information leak. An attacker who runs a concurrent, sandboxed application process on the user’s device can infer the nucleus size by indirectly measure the number of iterations of a certain loop, and thus fingerprint the input text. We use Flush+Reload [45] for our proof of concept, but the general approach works with any suitable side channel [17, 27, 31].

We design a fingerprint matching algorithm and show that (1) it tolerates noise in side-channel measurements, and (2) does not produce false positives. Therefore, an attacker can accurately identify the typed sequence out of many billions of possible candidates in an “open-world” setting, without assuming *a priori* that the user’s input belongs to a known small dataset. This technique can help de-anonymize text by asynchronously matching fingerprints collected from the user’s device to anonymous blog entries, forum posts, emails, etc. For example, we show that many of the anonymous users’ posts on the infamous Silk Road forum have unique fingerprints.

We conclude by explaining how to mitigate the information leak and discuss the importance of removing insecure coding patterns such as input-dependent loops from ML building blocks.

2 Background

2.1 Text generation via language model sampling

Let \mathbb{D} be a dictionary, $\mathbb{S} = \cup_{i \in \mathbb{N}} \mathbb{D}^i$ a set of possible *texts* (sequences of dictionary words), and $X \in \mathbb{S}$. A *language model* $\mathcal{M} : \mathbb{S} \rightarrow \mathbb{R}^{|\mathbb{D}|}$ maps a “prefix” $(x_1, \dots, x_n) \in \mathbb{S}$ to a probability distribution $(p_1, \dots, p_{|\mathbb{D}|})$ of the next word. **Text auto-completion** is a popular application of language generation. As the user is typing some text $X \in \mathbb{S}$, a language model is sampled at each time step $t \in \{1, \dots, |X|\}$, to generate a “probable” suffix for $X[:t]$ (the prefix of X up to index t).

Pure sampling draws the next word y according to the probabilities given by $\mathcal{M}(x_1, \dots, x_n)$, then invokes \mathcal{M} on (x_1, \dots, x_n, y) , and so on. Typically, sampling stops when a special end-of-sequence or end-of-sentence token is sampled, or when the probability of the entire sampled sequence (estimated by multiplying the model’s output probabilities for the sampled words) drops below a certain threshold. Other approaches include *greedy* sampling, which simply sets $x_{n+1} \leftarrow \operatorname{argmax} \mathcal{M}(x_1, \dots, x_n)$, and *top-k* sampling, which selects words corresponding to the top k highest values in $\mathcal{M}(x_1, \dots, x_n)$ and applies pure sampling to them according to their probabilities (normalized to sum up to 1). Different sampling methods generate text with different properties [19, 41]. Pure sampling produces poor-quality text (often, incomprehensible gibberish) as perceived by humans, while greedy sampling results

in a lack of language diversity, often with highly unnatural repetition.

Nucleus sampling [19] is similar to top-k sampling but instead of choosing candidates based on ranks, it chooses the maximal set (“nucleus”) of top-ranked words such that the sum of their probabilities is $\leq q$. It produces high-quality, high-diversity text [19] and performs well on metrics, including the Human Unified with Statistical Evaluation (HUSE) score [18].

2.2 Microarchitectural side channels

Process isolation in modern systems is a leaky abstraction. If a user’s process and an attacker’s concurrent process share physical hardware resources, the attacker can infer information about the user’s activity by analyzing contention patterns on the cache (see below), cache directories [43], GPU [29], translation lookaside buffer [15], and many other resources. These attacks, known as *microarchitectural side channels*, can be exploited by any untrusted, low-privilege process. Side-channel attacks have been demonstrated on many PC and mobile [27] platforms, and even from Javascript or WebAssembly code within the highly restricted browser sandbox [14, 30].

Several programming patterns are especially vulnerable to side-channel attacks. Loop arguments are a textbook example [26]: loops take longer to execute than non-iterative code, their execution time can be inferred using coarse timers, and their side effects on microarchitectural resources are repeated many times, amplifying the signal. Loops whose iterations depend on some secret can leak this secret through many microarchitectural [15, 28, 45] and physical [12, 13] side channels.

Cache side channels. Cache memory is shared even among isolated processes. When the contents of physical memory addresses are loaded or evicted by any process, it affects how fast that memory can be accessed by other processes. Therefore, memory access times measured by one process can reveal which memory addresses are accessed by another process. Cache attacks have been used to extract cryptographic keys [7, 28, 31, 32, 45, 47], steal login tokens [36], defeat OS security mechanisms [25], sniff user inputs [27], and more [35, 47, 48].

Flush+Reload [17, 45] is a popular type of cache attacks. When a victim process and a concurrent attacker process load the same shared library or a file, a single set of physical memory addresses containing the file’s content is mapped into both processes’ virtual address space. In this situation, the attacker can (1) cause the eviction of a specific memory address (“flush”), (2) wait, and (3) reload this memory address. Short reload time reveals that the victim has accessed this address after the eviction but before the load. If memory addresses monitored by the attacker do not contain shared memory, other cache attacks such as Prime+Probe [31, 32] may be used instead.

3 Fingerprinting auto-completed text sequences

Consider a text auto-completion assistant that uses nucleus sampling (see Section 2.1). At each step t , the user has typed $X[:t]$. The assistant uses $\mathcal{M}(X[:t])$ to generate nucleus q and samples from it to auto-complete the user’s text. We assume that the assistant stops

sampling at the end of every sentence and resets. Let $\mathcal{I}_{\mathcal{M},q}(X) \in \mathbb{R}^{|X|}$ be the *nucleus size series* (NSS) generated by the above procedure. Figure 1 shows an example.

3.1 Fingerprints of text sequences

Let $X, Y \in \mathbb{S}$ be text sequences s.t. $|X| = |Y|$. We say that X and Y are *similar* if they have identical subsequences of length N starting at the same index, i.e., $\exists i \in \mathbb{Z}$, $0 \leq i < |X| - N$ s.t. $X[i : i + N] = Y[i : i + N]$. We set $N = 50$, which is a very rigorous criterion for similarity: if two sequences have a common 50-word subsequence in exactly the same position, they are likely identical or have some identical source (and are thus *semantically* close to each other).

Let π be a procedure that receives as input $X \in \mathbb{S}$ and returns a vector in $\mathbb{R}^{|X|}$. We say that $\pi(X)$ is a **fingerprint** if there exists a monotonically increasing *uniqueness radius* $U : \mathbb{N} \rightarrow \mathbb{R}$ such that for any $Y \in \mathbb{S}$ which is not similar to X and $|Y| = |X|$, $\|\pi(X) - \pi(Y)\| > U(|X|)$ where $\|\cdot\|$ is the Euclidean norm. In other words, there exists a “ball” around the fingerprint of any sequence X such that no other sequence has its fingerprint within that ball (unless it is similar to X). This defines an *open-world* fingerprint, i.e., the uniqueness of a sequence’s fingerprint holds with respect to all natural-language sequences and not just a specific dataset.

3.2 Nucleus size series is a fingerprint

We conjecture that $\pi(X) = \mathcal{I}_{\mathcal{M},q}(X)$ of any English sequence is a fingerprint, as long as $\mathcal{I}_{\mathcal{M},q}(X)$ is sufficiently “variable.” We define variability of $\mathcal{I}_{\mathcal{M},q}(X) = (n_1, \dots, n_{|X|})$ as $\sqrt{\frac{1}{|X|} \sum_{i=1}^{|X|} (n_i - \mu)^2}$, where $\mu = \frac{1}{|X|} \sum_{i=1}^{|X|} n_i$ (by analogy with statistical variance). We say that X is *variable* if variability of its NSS is greater than some $T \in \mathbb{R}$. T depends on the language model \mathcal{M} , and is set to 1450 in our experiments.

It is computationally infeasible to compute $\|\pi(X) - \pi(Y)\|$ for every pair $X, Y \in \mathbb{S}$ in the English language. To validate our conjecture, we show that when a “variable” X and another sequence Y are sampled from a real-world English corpus and X and Y are not similar, it always holds that $\|\pi(X) - \pi(Y)\| > U(|X|)$ for a large $U(|X|)$. Critically, U depends only on the sequence length but not the size or domain of the corpus from which X is drawn. Furthermore, this holds for **any** Y , variable or not. This implies that there are no other fingerprints within the U -radius ball of $\pi(X)$.

Generating NSS. We downloaded 5 “subreddit” archives from Convokit [8] that have the fewest common users: asoiaf, india, OkCupid, electronic_cigarette, and Random_Acts_of_Amazon. We also downloaded the sports subreddit that has more active users and posts. We then aggregated each user’s posts into longer sequences (up to 3000 words) by concatenating them in chronological order.

To simulate auto-completion running in the background while a text sequence is being typed, we invoke Hugging Face Transformers language generator (`run_generation.py`) to drive a GPT-2 [34] language model (`gpt2-small`) and output one word for every prefix.

We use nucleus size with $q = 0.9$. To reduce computational complexity, we modified the script to save the encoder’s hidden state for every prefix, so it is necessary to decode only one additional word for the next prefix.

Many sequences are variable. The fraction of variable sequences depends on the domain: 43.6% for the OkCupid dataset, 62.8% for asoiaf, 77.6% for india, 71.6% for electronic_cigarette, 41.6% for Random_Acts_Of_Amazon, 42% for sports. Variability seems to be strongly and inversely correlated with the average sentence length, i.e., short sentences result in high variability. We conjecture that the (re-initialized) language model is more “uncertain” about the next word at the beginning of sentences, and large nucleus sizes correspond to high variability. Figure 1 illustrates this effect.

NSS of a variable sequence is unique. We measure pairwise Euclidean distances between the NSS of variable sequences and the NSS of other (not necessarily variable) sequences. Figure 2a shows the histogram (smoothed by averaging over a 10-bucket window) for 500 randomly chosen 2700-word sequences from the OkCupid dataset. Sample density decreases exponentially with distance from the density peak, which is around 105k. Because we omit the pairs where neither NSS is variable, this effect is asymmetric: density decreases slower above the peak than below the peak. Exponential decay to the left ensures that the lowest values observed in practice are never too far from the peak.

To verify this on a larger scale, we confirmed that the lowest pairwise distance between a variable NSS and any other NSS is consistent regardless of the dataset size (Figure 2b) or domain (Figure 2c).

Algorithm 1 Nucleus sampling [24]

```

1: procedure SAMPLE_SEQUENCE( $\mathcal{M}, p, X$ )
2:    $logits \leftarrow \mathcal{M}(X)$  // get logits
3:    $logits \leftarrow \text{TOP\_P\_FILTERING}(logits, p)$ 
4:    $next \leftarrow \text{MULTINOMIAL\_SAMPLE}(logits)$ 
5:   return  $next$ 
6:
7: procedure TOP_P_FILTERING( $logits, p$ )
8:    $sorted\_logits, indices \leftarrow \text{DESCEND\_ARGSORT}(logits)$ 
9:    $cum\_probs \leftarrow \text{CUM\_SUM}(\text{SOFTMAX}(sorted\_logits))$ 
10:   $not\_in\_p \leftarrow []$ 
11:  for  $i \in \{1 \dots \text{LEN}(logits)\}$  do
12:    if  $cum\_probs[i] > p$  then
13:       $not\_in\_p.APPEND(indices[i])$ 
14:  for  $i \in not\_in\_p$  do ← number of iterations
15:     $logits[i] \leftarrow -\infty$  corresponds to nucleus
size
16:  return  $logits$ 

```

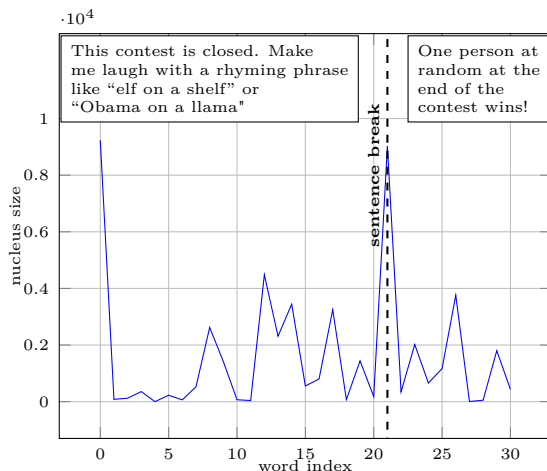
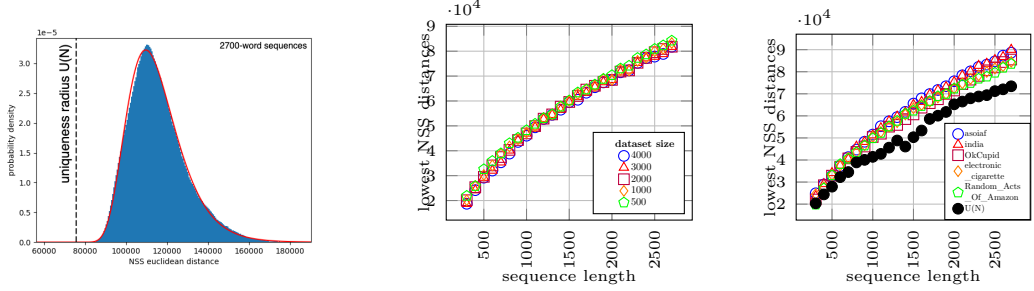


Figure 1: NSS of a two-sentence sequence.

NSS of a variable sequence is a fingerprint. To formally satisfy our definition of a fingerprint, NSS of variable sequences must have a uniqueness radius that depends on N .



(a) NSS pairwise distances for 500 random sequences (OkCupid). (b) Lowest NSS distances for different dataset sizes (sports). (c) Lowest NSS distances for different domains.

Figure 2: Nucleus size series (NSS) are fingerprints.

To show this for a given N , we take the dataset with the lowest average variability and fit a log-normal distribution, which is the best fit among 90 distributions [10], to its sample histogram, as shown in Figure 2a. We chose $U(N)$ such that, on our fitted distribution, the probability to sample an element lower than $U(N)$ is $\epsilon \equiv 10^{-18}$, which we consider negligible. Figure 2c shows $U(N)$ for various N .

3.3 Execution path of nucleus sampling reveals nucleus sizes

Algorithm 1 shows the pseudo-code of nucleus sampling. After obtaining the probability of each possible next token from the language model, it calls `TOP_P_FILTERING`, which sorts and sums up the probabilities. It then selects the tokens whose cumulative probability is outside top_p and sets the corresponding logits to $-\infty$, i.e., removes these tokens. If an adversary can infer the number of loop iterations in line 14, he can learn the number of tokens removed from the vocabulary and thus the nucleus size, which is equal to the vocabulary size minus the number of removed tokens.

Auto-completion exposes not just the nucleus size at each step, but also the number of completed words before it stops due to low probability or end-of-sequence token. The series of these numbers, in addition to nucleus sizes, may be an even stronger fingerprint, but we leave this to future work.

4 Attack overview

4.1 Threat model

Consider a user who types text into a program that uses an auto-completion assistant based on nucleus sampling. At the same time, an attacker is running a concurrent, low-privilege process on the user’s machine, (e.g., inside another application). The input into auto-completion does not leave the assistant’s internal memory. Memory isolation and sandboxing ensure that the attacker’s process cannot directly access this memory, nor view

the user’s keyboard entries.

The attacker’s goal is to infer the nucleus size series, which are revealed through a loop iteration count (see Section 3.3), via any available side channel (see Section 2.2). We assume that the attacker’s measurement of the side channel is “aligned,” i.e., the attacker can determine when the language model is queried to auto-complete a prefix (inferring this is relatively straightforward—see Section 5.1). The measurement can be imprecise, but we show that the error is bounded (see Appendix A).

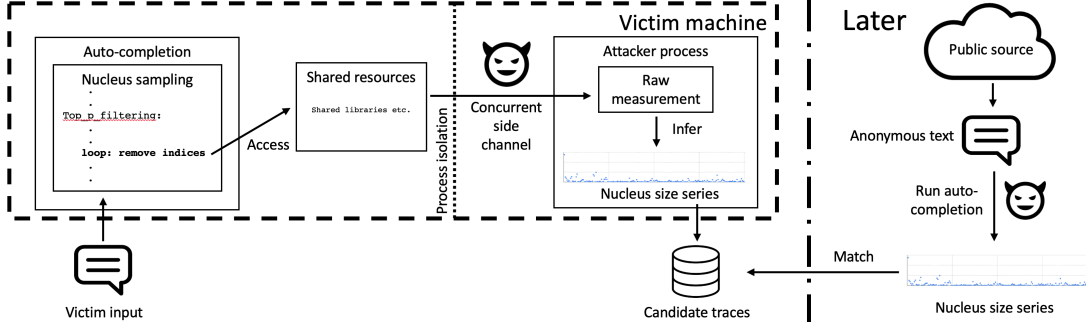


Figure 3: Attack overview.

One application of this attack is de-anonymization (see Figure 3). Consider a user who anonymously publishes some text on Reddit, Twitter, a blog, or a “Dark Web” cybercrime forum. In the *online phase* of the attack, while the user is typing, the attacker collects a trace by measuring the available side channel. The attacker stores all traces, along with user identifiers such as the IP address of the machine where the trace was collected. In a later, *offline phase*, the attacker obtains anonymously published texts and attempts to match them against the collected traces.

4.2 Matching an anonymous text to a side-channel trace

We assume that the attacker has access to the same language-model implementation as used by the victim; this is common for popular, publicly released models and implementations such as GPT-2 and Hugging Face. Therefore, for any text, the attacker can reproduce the corresponding nucleus size series by re-running the model on the prefixes of this text.

Algorithm 2 shows how the attacker can match a sequence against (previously collected) candidate traces. The algorithm first generates the nucleus size series of the sequence. If the sequence is sufficiently long and variable (see Section 3.2), the algorithm computes the distance from every candidate trace to the nucleus size sequence. If the distance is under some threshold τ_N that depends on the length N of the sequence, the algorithm declares a successful match.

Generating a list of traces. $\text{GENTRACES}(\text{candidate_traces}, |X|)$ returns a list of traces whose length is equal to X that the attacker wants to de-anonymize. To create this list,

the attacker drops all traces shorter than $|X|$ and, for longer traces, he can consider all contiguous sub-traces of length $|X|$.

Choosing τ_N to ensure no false positives. Let $\mathbb{V} \subseteq \mathbb{S}$ the set of texts whose NSS is variable, $X \in \mathbb{V}$ a variable text, and $Y \in \mathbb{S}$ any text s.t. X, Y have the same length N but are not similar. Let t be a trace measured while the user was typing Y . We want to avoid false positives, i.e., Y 's trace mistakenly matched to X : $\|\mathcal{I}_{\mathcal{M},q}(X) - t\| < \tau_N$. Let T^Y be the probability distribution of traces measured while the user is typing Y , and let $d(N)$ be the bound on the attacker's measurement error:

$$Pr_{t \leftarrow T^Y} [\|\mathcal{I}_{\mathcal{M},q}(Y) - t\| < d(N)] \geq 1 - \epsilon \quad \text{for some small } \epsilon \quad (1)$$

From Section 3.2, we have that, for uniformly sampled X and Y ,

$$Pr_{X,Y \leftarrow \mathbb{V} \times \mathbb{S}} [\|\mathcal{I}_{\mathcal{M},q}(Y) - \mathcal{I}_{\mathcal{M},q}(X)\| > U(N)] \geq 1 - \epsilon \quad (2)$$

For any t, X, Y such that the events in Equations 1 and 2 hold, the distance from t to X 's fingerprint is bound by the triangle inequality: $\|\mathcal{I}_{\mathcal{M},q}(X) - t\| \geq U(N) - d(N)$ —see Figure 4. By setting the threshold $\tau_N \leftarrow U(N) - d(N)$, we guarantee that for random $X \in \mathbb{V}$ and $Y \in \mathbb{S}$, the probability of a false positive where $\|\mathcal{I}_{\mathcal{M},q}(X) - t\| < \tau_N$ is at most 2ϵ (by union bound).

Beyond distance-based matching. Our matching algorithm is simple, very conservative, and amenable to theoretical analysis. A real-world attacker who is not interested in provable guarantees could use much more sophisticated methods instead. Convolutional neural networks often outperform distance-based methods [37, 39], especially with noisy measurements [37]. For our task, these methods are likely to be effective even when using a very noisy side channel where $d(N)$ is higher than $U(N)$. Empirically demonstrating their precision for time-series fingerprint matching with an extremely low base rate [4] would take many billions of measurements, however.

Algorithm 2 Matching a sequence to traces

```

1: procedure MATCHING( $X, candidates$ )
2:    $\mathcal{I}_{\mathcal{M},q}(X) \leftarrow \text{FIND\_NSS}(\mathcal{M}, q, X)$ 
3:   if  $\mathcal{I}_{\mathcal{M},q}(X)$  not variable then
4:     return not_variable
5:   for  $t \in \text{GENTRACES}(candidates, |X|)$  do
6:     if  $\|\mathcal{I}_{\mathcal{M},q}(X) - t\| < \tau_{|t|}$  then
7:       return  $t$ 
8:   return no_match

```

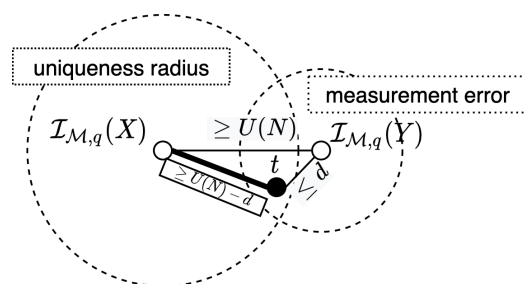


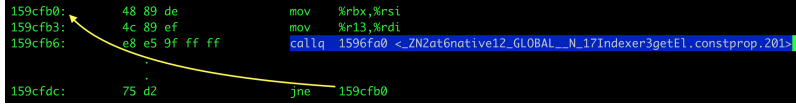
Figure 4: Bound on measurement error and uniqueness radius ensures no false positives.

5 Fingerprinting via a cache side channel

Our proof of concept uses a Flush+Reload attack (see Section 2.2). For this attack, we show that the noise $d(N)$ of the attacker’s measurements of nucleus sizes is much smaller than the uniqueness radius $U(N)$ of nucleus size series. This attack thus has high recall and **no false positives** (see Section 4.2). We also demonstrate that **uniqueness radius grows faster than measurement noise** as a function of the sequence length N . Therefore, even for noisier measurements from a different side channel, machine, or software setup, we expect that there exists an N such that $U(N) \gg d(N)$.

5.1 Experimental setup

Our “victim” uses an auto-completion app based on Hugging Face’s PyTorch code driving a GPT-2-small language model, as in Section 3.2. We used Hugging Face [23] and Pytorch [33] code versions from, respectively, 7/18/2019 and 7/22/2019. The victim and attacker run as (isolated) processes on the same core of an 8-core, Intel Xeon E5-1660 v4 CPU. The victim, like any process that uses PyTorch, loads the shared object (*SO*) `libtorch.so` into their process. This SO is in a public, world-readable directory, as long as PyTorch is installed on the machine. Our attacker loads the same SO file into their process. Consequently, the physical memory addresses that contain the SO are mapped into the virtual process space of both the attacker and the victim (operating systems have a copy-on-write policy for SOs in the physical memory). The attacker uses Flush+Reload to monitor the first instruction of a function called within the loop, as shown in Figure 5.



```

159cfb0: 48 89 de      mov    %rbx,%rsi
159cfb3: 4c 89 ef      mov    %r13,%rdi
159cfb6: e8 e5 9f ff   callq 1596fa0 <_ZN2at6native12_GLOBAI...N_17Indexer3getEl.constprop.201>
          .
          .
159cfdc: 75 d2        jne    159cfb0

```

Figure 5: Assembly code of the loop in lines 14-15 of Algorithm 1, implemented in `libtorch.so`.

To determine when typing starts or ends, the attacker can use any side channel from Section 2.2 to probe the auto-completion application or shared libraries. For segmenting the trace into prefixes, the attacker can use CPU timestamps for each Flush+Reload hit to identify the gaps. If the user deletes some words as he types, the trace will not match the fingerprint exactly (this may cause false negatives but not false positives). The attacker can detect deletions by shifting the trace by n words and matching a part of the shifted trace against the fingerprint until the distance is small for some n .

Before measured traces can be used, they must be processed to remove noise and outliers—see Appendix A.

5.2 Measurement error and attack recall

The analysis in Section 4.2 assumes that the side-channel measurement error is bounded by some $d(N)$. After measuring 1566 traces from the reddit-sports dataset and removing

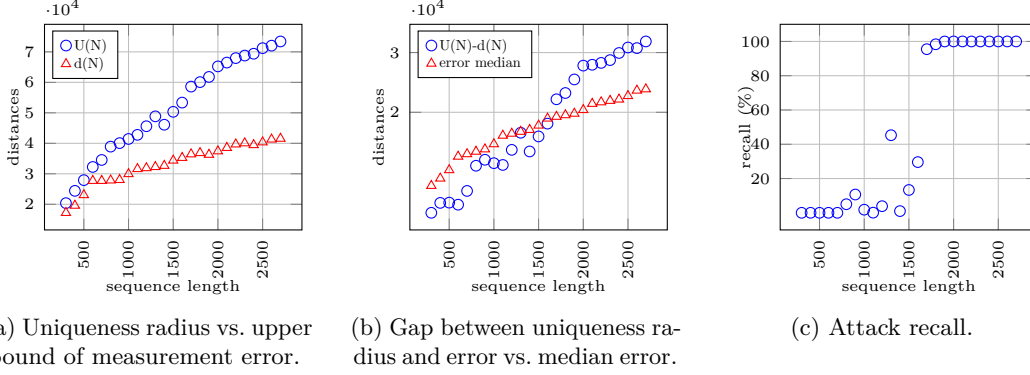


Figure 6: Measurement error and attack recall.

noisy traces, we fit a normal distribution and set $d(N)$ to 10 standard deviations above the mean, thus the probability that measurement error exceeds $d(N)$ is under $\epsilon = 10^{-18}$. Figure 6a shows $d(N)$ as a function of N , and how the uniqueness radius $U(N)$ diverges from $d(N)$.

This illustrates the fundamental characteristic that enables our attack: **pairwise distances between fingerprints grow faster as a function of sequence length N than the attacker’s measurement error**. Therefore, if a sequence is long enough, the attacker can match its fingerprint without false positives. This property can hold for any side channel, not just Flush+Reload we use in our experiments. The key observation is that the (squared) error of a single measurement is, on average, smaller than the (squared) difference between two different nucleus sizes.

In Algorithm 2, we set the threshold τ_N to $U(N) - d(N)$, so that the recall is equal to the probability that measurement error is below $U(N) - d(N)$. Figure 6c shows recall for different N ; when $N \geq 1900$, the recall of our attack is greater than 99%.

5.3 Case study: Silk Road forum

To show that users of a real-world anonymous forum would have been vulnerable if they had used auto-completion based on nucleus sampling, we used 41 users from the Silk Road archive [38] who had over 2700 words in their posts. For each such user, we concatenated their posts in chronological order into a single sequence and generated the corresponding NSS fingerprint.

We simulated the auto-completion process for each user’s sequence using the Hugging Face Transformers language generator and applied our proof-of-concept attack from Section 3.2. In reality, posts may be separated by unrelated typing, but (a) it is relatively straightforward to identify the current application via techniques from Section 2.2, and (b) the attacker knows when the typing begins and ends (see Section 5.1). To ensure even stronger isolation, we ran the attack process in an AppArmor [1] sandbox (by default, it

still lets the attacker read PyTorch shared objects). These experiments were done on the same machine as in Section 5.1.

We truncated all traces to $N=2700$ and filtered out NSS that are not sufficiently variable. This left 18 users out of 41. For each of them, we computed the measurement error of the attack, i.e., the distance between the measured trace and NSS—see Appendix B. In all cases, the error is less than $U(N) - d(N)$, thus the attack would have been able to correctly de-anonymize these 18 users with no false positives or false negatives.

6 Mitigation

Algorithm 3 is our suggested replacement for Algorithm 1. It follows two standard guidelines for cryptographic code: (1) it avoids data-dependent memory accesses at a granularity coarser than a cache line [6, 16], and (2) its execution time is not correlated with secret data [11]. Figures 7a and 7b show the relationship between the nucleus size and execution time of the token removal loop with and without the mitigation, indicating that our implementation reduces the correlation due to the fixed number of iterations.

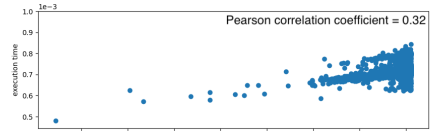
The cost of our mitigation is a 1.15x average slowdown in the loop execution time, which translates into only a 0.1% increase in the runtime of `SAMPLE_SEQUENCE` (which itself accounts for a tiny fraction of the execution time relative to the encoder/decoder passes). When simulating auto-completion on a 2700-word sequence in the setup from Section 5.1, there was a negligible, 0.3% runtime difference in favor of our algorithm, implying that the difference between Algorithms 1 and 3 is dominated by other factors, such as natural fluctuations in the CPU load.

Algorithm 3 Top-p filtering with a fixed number of loop iterations.

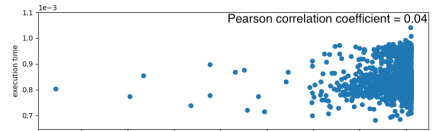
```

1: procedure TOP_P_FILTERING(logits, p)
2:   sorted_logits, indices  $\leftarrow$  DESCENDING_ARGSORT(logits)
3:   cum_probs  $\leftarrow$  CUM_SUM(SOFTMAX(sorted_logits))
4:
5:   for  $i \in \{1 \dots \text{LEN}(\text{logits})\}$  do
6:      $z \leftarrow \text{FLOAT}((\text{cum\_probs}[i] > p)) \cdot \text{MAX\_FLOAT}$ 
7:     logits[indices[i]]  $\leftarrow$  logits[indices[i]] - z
8:
9:   return logits

```



(a) Nucleus size vs. run time (original)



(b) Nucleus size vs. run time (mitigation)

Figure 7: Execution time of the token removal loop with and without the mitigation.

No implementation is immune to side channels, however. Address bits within a cache line could still leak through the cache on certain processors [46]. Even without input-dependent paths, loop runtimes may still slightly depend on the input due to value-dependent

execution times of floating-point operations [3] (an attacker must be able to measure the loop very accurately to exploit this). Mitigations of these and other side-channel risks incur implementational and runtime overheads [11].

We believe that our implementation strikes a good balance by substantially increasing the gap between what side-channel attacks can achieve on specific platforms in controlled laboratory conditions vs. what is available to real-world attackers. We argue that removing “easy” targets like input-dependent loops should be a minimal security standard for core ML building blocks.

7 Related work

Prior work showed how to infer model architectures and weights—but not *inputs*—via model execution time [9], addresses of memory accesses leaked by GPUs [21] and trusted hardware enclaves [22], and or via cache [20, 44] and GPU [29] side channels.

The only prior work on inferring model inputs required hardware attacks, such as physically probing the power consumption of an FPGA accelerator [40], physically probing an external microcontroller executing the model [5], or inferring coarse information about the input’s class from hardware performance counters [2]. To the best of our knowledge, ours is the first work to show the feasibility of inferring neural-network inputs in a conventional, software-only setting, where the attacker is limited to executing an isolated malicious application on the victim’s machine.

8 Conclusions

We used nucleus sampling, a popular approach for text generation, as a case study of ML systems that unwittingly leak their confidential inputs. As our main technical contribution, we demonstrated that the series of nucleus sizes associated with an English-language word sequence is a fingerprint which uniquely identifies this sequence. We showed how a side-channel attacker can measure these fingerprints and use them to de-anonymize anonymous text. Finally, we explained how to mitigate this leak by reducing input-dependent control flows in the implementations of ML systems.

Acknowledgments and Disclosure of Funding

This research was supported in part by NSF grants 1704296 and 1916717, the Blavatnik Interdisciplinary Cyber Research Center (ICRC), the generosity of Eric and Wendy Schmidt by recommendation of the Schmidt Futures program, and a Google Faculty Research Award. Roei Schuster is a member of the Check Point Institute of Information Security.

References

- [1] AppArmor. <https://gitlab.com/apparmor/apparmor/-/wikis/home>, 1998. accessed: May 2020.

- [2] M. Alam and D. Mukhopadhyay. How secure are deep learning algorithms from side-channel based reverse engineering? In *DAC*, 2019.
- [3] M. Andryscio, D. Kohlbrenner, K. Mowery, R. Jhala, S. Lerner, and H. Shacham. On subnormal floating point and abnormal timing. In *S&P*, 2015.
- [4] S. Axelsson. The base-rate fallacy and the difficulty of intrusion detection. *TISSEC*, 3(3):186–205, 2000.
- [5] L. Batina, S. Bhasin, D. Jap, and S. Picek. CSI neural network: Using side-channels to recover your artificial neural network information. In *USENIX Security*, 2019.
- [6] E. F. Brickell. Technologies to improve platform security. In *CHES*, 2011.
- [7] S. Cohnsey, A. Kwong, S. Paz, D. Genkin, N. Heninger, E. Ronen, and Y. Yarom. Pseudorandom black swans: Cache attacks on CTR DRBG. In *S&P*, 2020.
- [8] ConvoKit. Cornell conversational analysis toolkit. <https://convokit.cornell.edu/>, 2020. accessed: June 2020.
- [9] V. Duddu, D. Samanta, D. V. Rao, and V. E. Balas. Stealing neural networks via timing side channels. *arXiv:1812.11720*, 2018.
- [10] Fit distribution module/script (fitdist). <https://github.com/alreich/fitdist>, 2020. accessed: June 2020.
- [11] Q. Ge, Y. Yarom, D. Cock, and G. Heiser. A survey of microarchitectural timing attacks and countermeasures on contemporary hardware. *Journal of Cryptographic Engineering*, 8(1):1–27, 2018.
- [12] D. Genkin, A. Shamir, and E. Tromer. RSA key extraction via low-bandwidth acoustic cryptanalysis. In *CRYPTO*, 2014.
- [13] D. Genkin, L. Pachmanov, I. Pipman, and E. Tromer. ECDH key-extraction via low-bandwidth electromagnetic attacks on PCs. In *CT-RSA*, 2016.
- [14] D. Genkin, L. Pachmanov, E. Tromer, and Y. Yarom. Drive-by key-extraction cache attacks from portable code. In *ACNS*, 2018.
- [15] B. Gras, K. Razavi, H. Bos, and C. Giuffrida. Translation leak-aside buffer: Defeating cache side-channel protections with TLB attacks. In *USENIX Security*, 2018.
- [16] S. Gueron. Efficient software implementations of modular exponentiation. *Journal of Cryptographic Engineering*, 2(1):31–43, 2012.
- [17] D. Gullasch, E. Bangerter, and S. Krenn. Cache games—bringing access-based cache attacks on AES to practice. In *S&P*, 2011.

- [18] T. B. Hashimoto, H. Zhang, and P. Liang. Unifying human and statistical evaluation for natural language generation. In *NAACL*, 2019.
- [19] A. Holtzman, J. Buys, M. Forbes, and Y. Choi. The curious case of neural text degeneration. In *ICLR*, 2020.
- [20] S. Hong, M. Davinroy, Y. Kaya, D. Dachman-Soled, and T. Dumitras. How to Own NAS in your spare time. In *ICLR*, 2020.
- [21] X. Hu, L. Liang, L. Deng, S. Li, X. Xie, Y. Ji, Y. Ding, C. Liu, T. Sherwood, and Y. Xie. Neural network model extraction attacks in edge devices by hearing architectural hints. In *ASPLOS*, 2020.
- [22] W. Hua, Z. Zhang, and G. E. Suh. Reverse engineering convolutional neural networks through side-channel information leaks. In *DAC*, 2018.
- [23] Hugging Face. Transformers on github. <https://github.com/huggingface/transformers>, 2020. accessed: June 2020.
- [24] Hugging Face. Write with Transformer (demo). <https://transformer.huggingface.co/>, 2020. accessed: June 2020.
- [25] R. Hund, C. Willems, and T. Holz. Practical timing side channel attacks against kernel space ASLR. In *S&P*, 2013.
- [26] P. C. Kocher. Timing attacks on implementations of Diffie-Hellman, RSA, DSS, and other systems. In *CRYPTO*, 1996.
- [27] M. Lipp, D. Gruss, R. Spreitzer, C. Maurice, and S. Mangard. Armageddon: Cache attacks on mobile devices. In *USENIX Security*, 2016.
- [28] F. Liu, Y. Yarom, Q. Ge, G. Heiser, and R. B. Lee. Last-level cache side-channel attacks are practical. In *S&P*, 2015.
- [29] H. Naghibijouybari, A. Neupane, Z. Qian, and N. Abu-Ghazaleh. Rendered insecure: GPU side channel attacks are practical. In *CCS*, 2018.
- [30] Y. Oren, V. P. Kemerlis, S. Sethumadhavan, and A. D. Keromytis. The spy in the sandbox: Practical cache attacks in JavaScript and their implications. In *CCS*, 2015.
- [31] D. A. Osvik, A. Shamir, and E. Tromer. Cache attacks and countermeasures: the case of AES. In *CT-RSA*, 2006.
- [32] C. Percival. Cache missing for fun and profit. <https://www.daemonology.net/papers/htt.pdf>, 2005.

- [33] PyTorch. <https://github.com/pytorch/pytorch>, 2020. accessed: June 2020.
- [34] A. Radford, J. Wu, R. Child, D. Luan, D. Amodei, and I. Sutskever. Language models are unsupervised multitask learners. *OpenAI Blog*, 1(8), 2019.
- [35] T. Ristenpart, E. Tromer, H. Shacham, and S. Savage. Hey, you, get off of my cloud: Exploring information leakage in third-party compute clouds. In *CCS*, 2009.
- [36] E. Ronen, R. Gillham, D. Genkin, A. Shamir, D. Wong, and Y. Yarom. The 9 lives of Bleichenbacher’s CAT: New Cache ATtacks on TLS implementations. In *S&P*, 2019.
- [37] R. Schuster, V. Shmatikov, and E. Tromer. Beauty and the Burst: Remote identification of encrypted video streams. In *USENIX Security*, 2017.
- [38] Silk Road | Users. <https://antiloop.cc/sr/users/>, 2020. accessed: June 2020.
- [39] P. Sirinam, M. Imani, M. Juarez, and M. Wright. Deep fingerprinting: Undermining website fingerprinting defenses with deep learning. In *CCS*, 2018.
- [40] L. Wei, B. Luo, Y. Li, Y. Liu, and Q. Xu. I know what you see: Power side-channel attack on convolutional neural network accelerators. In *ACSAC*, 2018.
- [41] S. Welleck, I. Kulikov, J. Kim, R. Y. Pang, and K. Cho. Consistency of a recurrent language model with respect to incomplete decoding. *arXiv:2002.02492*, 2020.
- [42] T. Wolf, L. Debut, V. Sanh, J. Chaumond, C. Delangue, A. Moi, P. Cistac, T. Rault, R. Louf, M. Funtowicz, and J. Brew. HuggingFace’s transformers: State-of-the-art natural language processing. *arXiv:1910.03771*, 2019.
- [43] M. Yan, R. Sprabery, B. Gopireddy, C. Fletcher, R. Campbell, and J. Torrellas. Attack directories, not caches: Side channel attacks in a non-inclusive world. In *S&P*, 2019.
- [44] M. Yan, C. Fletcher, and J. Torrellas. Cache telepathy: Leveraging shared resource attacks to learn DNN architectures. In *USENIX Security*, 2020.
- [45] Y. Yarom and K. Falkner. FLUSH+RELOAD: A high resolution, low noise, L3 cache side-channel attack. In *USENIX Security*, 2014.
- [46] Y. Yarom, D. Genkin, and N. Heninger. CacheBleed: a timing attack on OpenSSL constant-time RSA. *Journal of Cryptographic Engineering*, 7(2):99–112, 2017.
- [47] Y. Zhang, A. Juels, M. K. Reiter, and T. Ristenpart. Cross-VM side channels and their use to extract private keys. In *CCS*, 2012.
- [48] Y. Zhang, A. Juels, M. K. Reiter, and T. Ristenpart. Cross-tenant side-channel attacks in PaaS clouds. In *CCS*, 2014.

A Trace preprocessing

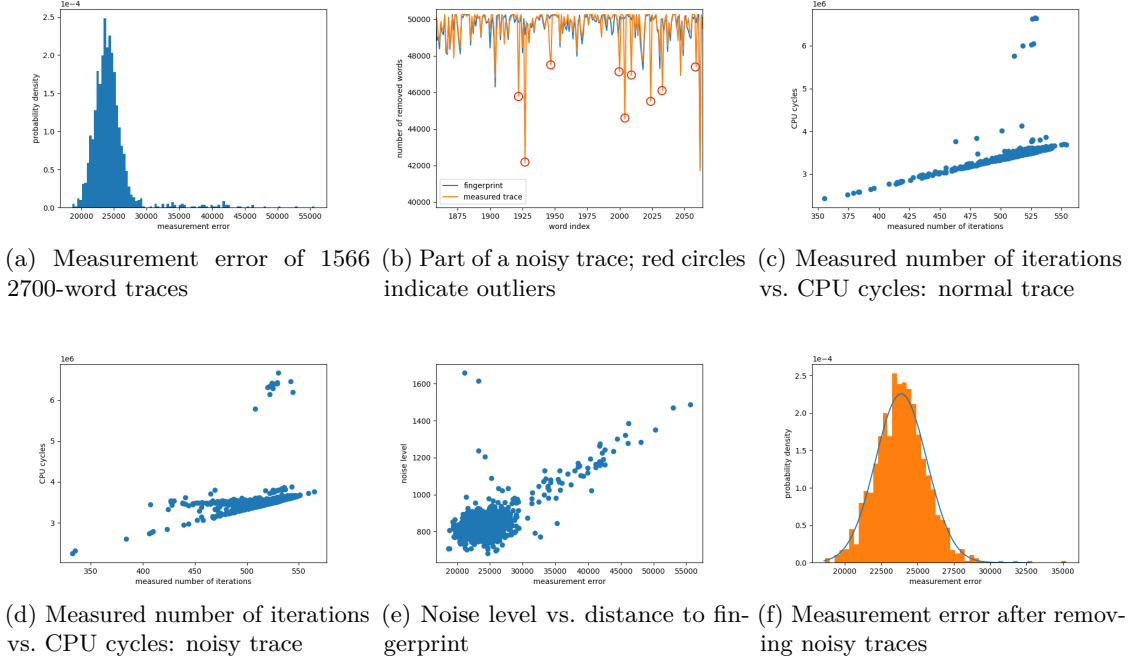


Figure 8: Filtering out noisy traces.

Challenge: loop iterations are faster than Flush+Reload. The attacker’s goal is to infer the number of iterations of the token removal loop (see Section 3.3). In the Reload phase of the Flush+Reload attack, the attacker learns whether the victim has accessed an address since it has been Flushed (see Section 2.2). A naive attack would iteratively perform Flush+Reload and receive indications whenever the victim accesses this address, which happens on every iteration of the target loop.

The problem is that Flushing and Reloading is two orders of magnitude slower than executing the target loop. If the victim performs more than one iteration per each attacker iteration, the attacker misses accesses. In our environment, the naive approach only captures a small fraction of the victim’s iterations. Fortunately, we observe that the fraction of the victim’s iterations captured by the attacker is consistently around 1.1%. Therefore, to estimate the actual number of iterations, the attacker can simply multiply the observed number by 100/1.1.

Challenge: some traces are very noisy. Figure 8a shows the distribution of measurement error over 1566 2700-word traces from the reddit-sports dataset. The distribution has a long tail due to several outliers where the error is very high. We observe (Figure 8b) that

outliers are associated with periods when the Flush+Reload loop was slower or produced more false negatives (an address access by the victim was not indicated by a lower load time). This can be due to high activity by concurrent processes sharing the attacker’s core, load on the cache bus, or other low-level interactions.

Filtering out noisy traces. We observe that in a normal state, the execution time of each iteration of the target loop is usually close to a constant. Figure 8c shows the relationship between the measured number of iterations and time (in CPU cycles). There are some outliers (likely caused by CPU interrupts), but the relationship is almost linear. If a trace is noisy, however, the correlation is weaker—see Figure 8d.

We measure the “noise level” of a trace as the mean squared distance of its (iterations, time) series relative to the expected line. Figure 8e shows the relationship between the noise level of a trace and the distance to its corresponding fingerprint. We filter out all traces whose noise above some threshold level. Figure 8f shows the histogram of measurement error after removing noisy traces.

In our experiments, we removed the noisiest 6% of the traces.

B Data for the Silk Road experiment

Table 1 shows variability and measurement error of nucleus size series corresponding to the posts of Silk Road forum users.

| user | variability | measurement error |
|----------------------|-------------|-------------------|
| cirrus | 1546.78 | 25635.48 |
| indica9 | 1763.87 | 22261.53 |
| stealth | 1455.91 | 24129.27 |
| cirrus(SR2) | 1753.64 | 20955.76 |
| jediknight | 1465.62 | 22010.80 |
| digitalalch | 1586.34 | 25537.31 |
| synergy | 1699.32 | 22907.05 |
| ssbd | 1701.14 | 23879.66 |
| captainwhitebeard | 2004.27 | 20950.86 |
| colorblack | 1502.06 | 20909.17 |
| nomad bloodbath | 2032.92 | 23724.85 |
| envious | 1504.53 | 22530.60 |
| modziw | 1737.35 | 21170.16 |
| v | 1586.50 | 21646.63 |
| sarge | 1522.02 | 20902.54 |
| warweed | 1667.98 | 22507.60 |
| samesamebutdifferent | 1521.18 | 21508.18 |
| scout | 1521.50 | 22985.98 |

Table 1: Variability and measurement error for Silk Road Forum users. (N is 2700, $U(N) - d(N)$ is 31860).